

Terahertz wave generation in orientation-patterned GaAs using resonantly enhanced scheme

K. L. Vodopyanov^{*a}, J.E. Schaar^a, P.S. Kuo^a, M.M. Fejer^a, X.Yu^b, J. S. Harris^b, V.G. Kozlov^c,
D. Bliss^d, C. Lynch^d

^a E. L. Ginzton Laboratory, Stanford University, Stanford, CA 94305, USA

^b Solid State Photonics Laboratory, Stanford University, Stanford, California 94305, USA

^c Microtech Instruments, Inc., Eugene, OR 97403, USA

^d Hanscom Air Force Research Laboratory, Bedford, Massachusetts 01731, USA

ABSTRACT

Zincblende semiconductors (GaAs, GaP) show great potential for quasi-phase-matched (QPM) THz generation because of their small (20 times less than in lithium niobate) absorption coefficient at terahertz frequencies, small mismatch between the optical group and THz phase velocities, high thermal conductivity, and decent electro-optical coefficient. Terahertz-wave generation was demonstrated recently in QPM GaAs, using optical rectification of femtosecond pulses. Here we report on a new efficient widely tunable (0.5-3.5 THz) source of THz radiation based on quasi-phase-matched GaAs crystal. The source is based on difference frequency generation inside the cavity of a synchronously pumped near-degenerate picosecond OPO and takes advantage of resonantly enhanced both the signal and the idler waves. THz average power as high as 1 mW was achieved in a compact setup.

Keywords: Terahertz waves, difference frequency generation, down-conversion, quasi-phase-matched, gallium arsenide, GaAs

1. INTRODUCTION

There is a potential for using terahertz (THz) waves ($1 \text{ THz} = 10^{12} \text{ Hz}$) for numerous applications including real-time imaging (THz waves have, in many occasions, much smaller scattering than the optical waves and thus can penetrate many materials) and rotational-vibrational spectroscopy, both in condensed and gaseous phase, because of richness of absorption spectra in the THz range. Parametric frequency down-conversion of optical pulses¹ is an established, but inefficient so far, way of generating terahertz radiation. Potentially, it allows attaining compact tunable THz emitters working at room temperature, by using wall-plug-efficient diode-pumped laser sources (most likely fiber lasers) with different temporal formats: from continuous-wave to femtosecond (fs) pulses. This technique can generate quasi-monochromatic THz radiation using difference frequency generation (DFG) with two laser input beams¹⁻⁶, or through THz-wave parametric oscillation⁷⁻⁹ with a single fixed-frequency optical pump. Alternatively, broadband THz transients can be generated by means of optical rectification (OR) of ultrashort (typically fs) laser pulses.¹⁰⁻¹³

There are however two significant factors which limit THz conversion efficiency in both OR and DFG, namely (1) conventional crystals used for THz generation (LiNbO₃, ZnTe) have high absorption at THz frequencies (characteristically $10\text{-}100 \text{ cm}^{-1}$), (2) there is a mismatch between propagation velocities of the THz wave packet and of the optical pulse which limits (especially in the OR case) the useful length of the crystal. As a result, optical-to-THz conversion efficiencies achieved so far are low¹⁴, typically $10^{-6}\text{-}10^{-9}$, even with femtosecond pump pulse energies as high as 10 mJ¹⁵. In order to enhance the optical-to-THz conversion efficiency, larger interaction lengths with collinear interaction of THz and optical waves is desirable. A way to solve the problem of propagation velocity mismatch and increase the interaction length, by means of using the tilted-front pump pulses, was demonstrated recently¹⁶. The authors reported conversion efficiency of 5×10^{-4} and achieved 240 μW THz average power from a bulk lithium niobate crystal when pumped by optical pulses from a Ti:Sapphire oscillator - regenerative amplifier system with 500 mW of average power at 1 kHz. Another approach to increase the efficiency of OR is to use quasi-phase-matched (QPM) nonlinear materials, as was first demonstrated with periodically-poled lithium niobate crystals (PPLN)^{17,18}. The authors used

femtosecond pulses at 800 nm and PPLN crystal with different QPM periods and achieved $\sim 10^{-5}$ conversion efficiency. PPLN was cryogenically cooled ($T=18$ K) to reduce THz absorption.

Lately, THz-wave generation was demonstrated in QPM GaP¹⁹ and QPM GaAs²⁰⁻²¹. In fact, III-V semiconductors are very attractive for QPM THz-wave generation because of several appealing properties, namely (i) small THz absorption coefficient (smaller by more than one order of magnitude²² than in commonly used EO crystals: lithium niobate, ZnTe, CdTe, ZnSe), (ii) large coherence length due to small mismatch between the optical group and THz phase velocities, and (iii) high thermal conductivity. In Ref. 19, THz-waves were obtained by DFG in a periodically-inverted GaP stack, produced by direct-wafer-bonding technique, which was pumped with 10-nanosecond pulses near 1.55 μm . The authors of Ref. 20 produced THz output via OR using fs laser pulses and two different QPM GaAs structures: (i) diffusion-bonded stacked GaAs (DB-GaAs)²³ and (ii) epitaxially-grown orientation-patterned GaAs (OP-GaAs).²⁴ By changing the GaAs QPM period (504–1277 μm), or the pump wavelength (2–4.4 μm), tunable (0.9–3 THz) output was achieved with 3.3% quantum conversion efficiency and with only 2.3- μJ pump-pulse energy. When a compact Tm-based fs fiber laser with $\lambda \approx 2 \mu\text{m}$ and 100 MHz repetition rate was used as a pump source²¹, 3 μW of average THz power was generated in the OP-GaAs crystal at 1.8 and 2.5 THz.

2. QPM GAAS SAMPLES

We have used in this work three different types of QPM GaAs samples: (i) diffusion-bonded GaAs (DB-GaAs) produced by stacking and bonding together alternately rotated $\langle 110 \rangle$ GaAs plates; wafer fusion in this case creates a monolithic body with periodic change in the nonlinear coefficient, (ii) orientation-patterned GaAs (OP-GaAs) grown by a combination of molecular beam epitaxy, photolithography, and hydride vapor phase epitaxy (HVPE), where periodic inversions of the crystallographic orientation are grown into the material, and (iii) optically-contacted GaAs (OC-GaAs), which was similar to DB-GaAs since the technology involves separate plates of GaAs which are brought together with a 90° domain rotation between neighboring plates. Unlike DB-GaAs, the plates were not heated to create a uniform crystalline structure. The individual GaAs wafers were 5.08 cm (2") in diameter and 1 mm thick.

While DB-GaAs and OC-GaAs provide larger apertures, OP-GaAs (Fig. 1) has more reproducible technology and allows lithographic definition of QPM gratings. Also, OP-GaAs allows the most precise definition of periodic structure, however it suffers from limited aperture (height) of 0.4–0.8 mm.

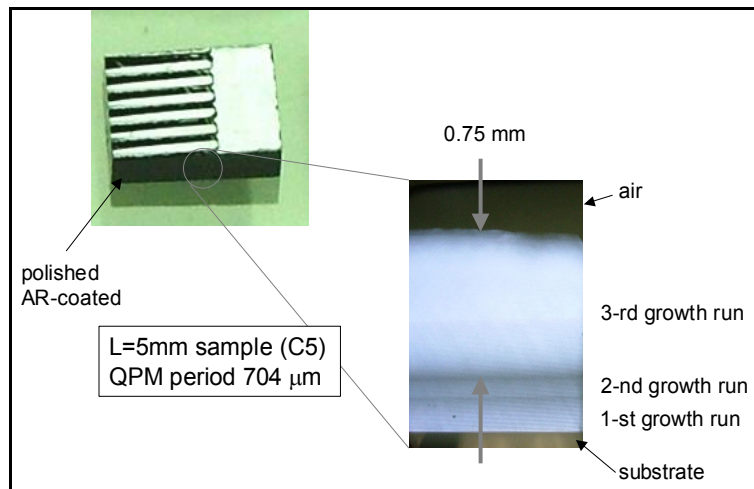


Fig. 1. OP-GaAs sample for the optical THz generation. The inset shows optical transmission obtained with a near-infrared ($\lambda \sim 1 \mu\text{m}$) microscope. There were 3 runs of HVPE thick-film growth, the last one being the most successful, providing the useful thickness of 0.75 mm.

3. DFG WITH PICOSECOND PULSES VS. OPTICAL RECTIFICATION WITH WITH FEMTOSECOND PULSES

Nonlinear optical frequency conversion is an intensity-dependent process and it might appear that, from the viewpoint of achieving high optical-to-THz efficiency, OR is more attractive than DFG, because of access to higher peak powers with fs pulses. Theoretical analysis of optical-to-THz conversion process in QPM electrooptical crystals²⁵ shows that for sufficiently short fs optical pulses (OR case), with $v_{THz}\tau \ll 1$, where τ is the optical pulsewidth and v_{THz} is the terahertz frequency, conversion efficiency does not depend on pulse duration. Furthermore, it has been shown that by mixing two bandwidth-limited picosecond (ps) pulses in the DFG scheme, one could achieve conversion efficiency, which is the same as in the case of fs pulses with the same fluence (or same pulse energy for the focused pump beams), provided that the picosecond pulse duration $\tau < L\Delta n / \sqrt{\pi}c$, where L is the length of the crystal, Δn is a mismatch between the optical group and THz refractive indices, and c is the speed of light. This condition corresponds to the case when the laser pulse duration is much shorter than the time walk-off, over the length of the crystal, between the optical pump and THz pulse. For a 1-cm-long GaAs, it corresponds to $\tau < 3.4$ ps (we assumed pump at 2.1 μm , so that $\Delta n \approx 0.18$). In essence, in the ps case, the length of coherent interaction between the optical and THz pulses is much longer than in the fs case, hence we get the same conversion efficiency despite of smaller peak intensity in the former case.

Therefore, to achieve high THz conversion efficiency (approaching Manley-Rowe limit), it is more advantageous to use DFG with ps pulses, in which case, the peak intensity (at the same fluence) is roughly two orders of magnitude smaller than in the case of fs pulses and allows avoiding parasitic high-order nonlinear effects (e.g. nonlinear refraction) which limit THz performance.^{20,26} However, for DFG one needs a two-color pump source.

4. NEAR-DEGENERATE SYNCHRONOUSLY-PUMPED PS OPO

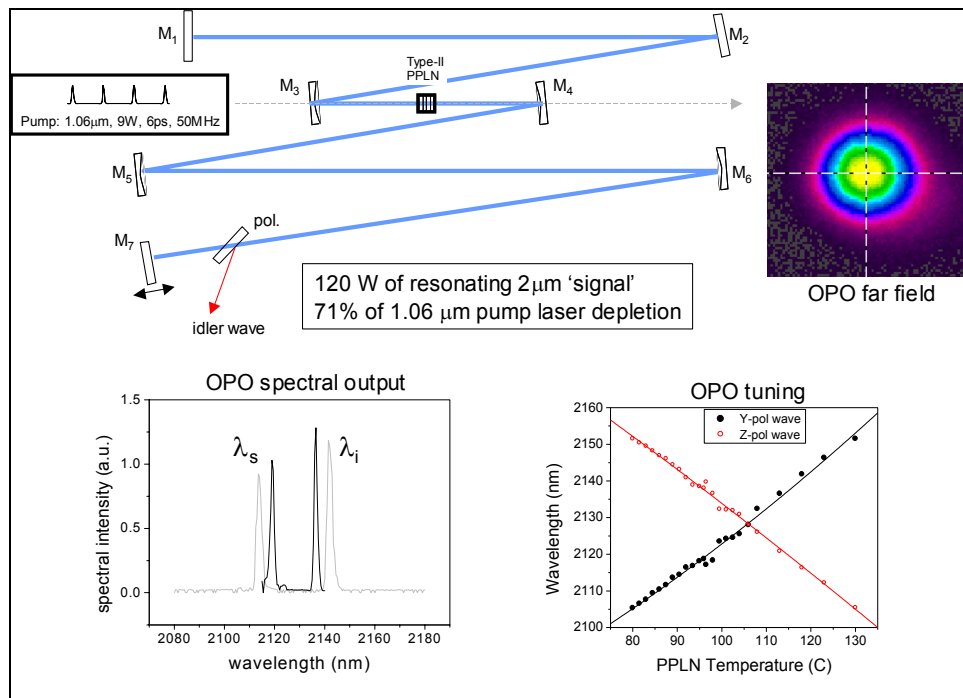


Fig. 2. Near –degenerate type-II PPLN OPO, synchronously pumped by ps pulses at 1.06 μm . Insets: ‘signal’ wave far field intensity distribution, spectral output of the OPO at two different PPLN temperatures, and OPO tuning curve with respect to PPLN temperature.

To generate two closely-spaced optical frequencies, we have used a near –degenerate type-II PPLN OPO, synchronously pumped by a CW mode-locked $Nd:YVO_4$ -laser at 1.064 μm (High Q Laser, Austria). The laser had repetition rate 50 MHz, pulse duration 7 ps, average power up to 10 W in a TEM_{00} mode. The PPLN crystal (HC Photonics) served as an OPO gain medium and was 10-mm-long, 3-mm-wide and 1-mm-thick and had a QPM period of 14.1 μm . It was designed for the type-II QPM three-wave interaction (Y-YZ), so that the signal and the idler had orthogonal polarizations. The PPLN was AR-coated for both 1.06 and 2.1–2.16 μm . The high-finesse standing-wave OPO cavity (Fig. 2) was 3-m-long and consisted of 7 mirrors, all of which were highly transmissive at 1.06 μm and highly reflective (>99.9%) in the vicinity of the 2.13 μm degeneracy wavelength. Mirrors M_1 - M_2 , and M_7 were flat, mirrors M_3 - M_4 had radius of curvature (ROC) of 200mm, and mirrors M_5 - M_6 - ROC of 500 mm. A polarizer inside the cavity served as a 100% idler-wave outcoupler, thus the OPO in this case was singly resonant (SRO).

Insets to Fig. 2 show (i) the signal-wave far field intensity distribution, (ii) spectral output of the OPO at two different PPLN temperatures, and (iii) OPO tuning curve with respect to the PPLN temperature. The OPO linewidth is preserved even when the OPO crosses the degeneracy point (at $\sim 106^\circ\text{C}$) and is close to the value of $\Delta\nu \sim 3\text{cm}^{-1}$ given by the time-bandwidth limit. In general, any frequency spacing, from 0 to 125 cm^{-1} (0–3.75 THz) between the OPO signal and the idler waves, can be achieved by changing the PPLN temperature.

At the measured pump beamsizes $w=30\mu\text{m}$ and the resonating signal eigenmode beamsizes of $w\sim 60\mu\text{m}$, the OPO threshold was $\sim 0.7\text{ W}$ and, at the full average pump power of 9 W available at the PPLN crystal, the idler output reached 3W with the pump depletion of 71%. By measuring the signal-wave power leaking through one of the OPO mirrors, we have measured that the intracavity resonating average signal power was as high as 120 W. Thus, there was a substantial resonant –field enhancement of the signal wave, due to low-loss cavity (the total round-trip loss was estimated to be 3%).

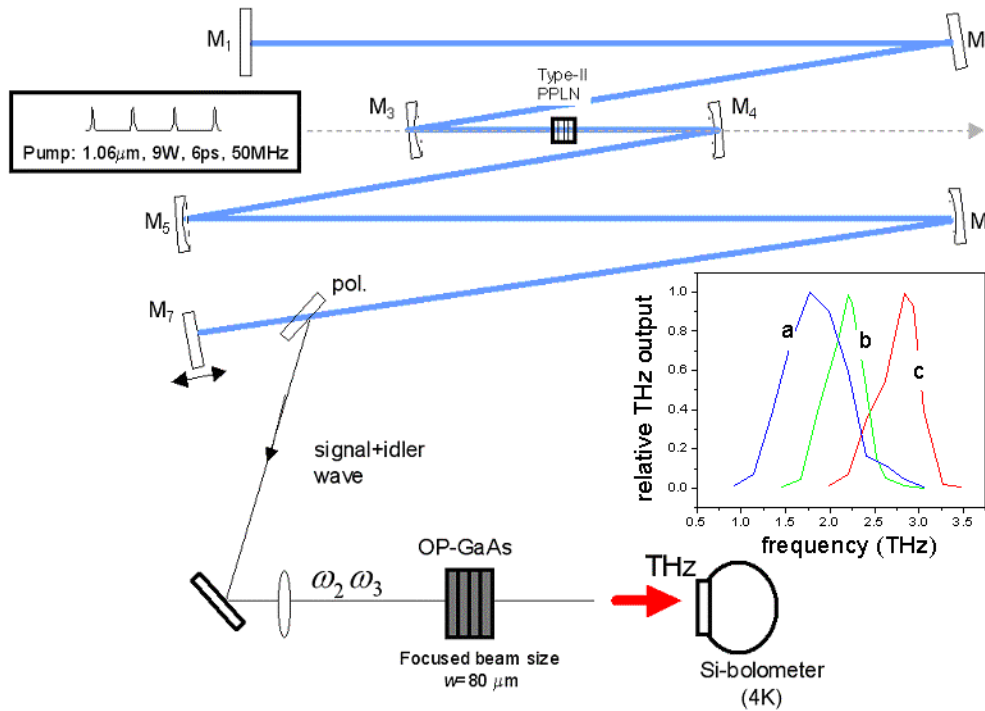


Fig.3. Experimental set-up for THz extracavity generation in QPM GaAs via DFG. A picosecond near –degenerate synchronously-pumped type-II PPLN OPO is used as a pump source. The inset shows THz output curves, as a function of THz frequency, for three OP-GaAs samples with QPM periods (lengths): (a) 932 μm ($L=3\text{ mm}$), (b) 759 μm ($L=10\text{ mm}$), and 564 μm ($L=5\text{ mm}$).

5. EXTRACAVITY THZ GENERATION

In our extracavity THz generation experiments, we used the signal and the idler waves of the OPO output (Fig. 3) to generate monochromatic THz output at their difference frequency. The two beams were collinearly focused into the GaAs crystal, to a beamsize of $\sim 80 \mu\text{m}$. The inset shows THz efficiency vs. frequency curves for three OP-GaAs samples with QPM periods of 932, 759 and 564 μm . For each sample, THz output is maximized when the THz frequency determined by the beat note between the two optical frequencies $\omega_{\text{THz}} = \omega_3 - \omega_2$, matches the QPM condition. Here ω_3 and ω_2 are angular frequencies of the OPO signal and the idler. THz tuning curves obtained in this experiment (THz peak frequency vs. GaAs QPM period, Fig. 4) are in excellent agreement with our OR results with fs pulses²⁰.

Fig.5 is a log-log plot of THz average power versus average pump power for a 5-mm-long OP-GaAs sample with the QPM period 704 μm and the central frequency of 2.2 THz. In fact, the powers at the two pump beams (the OPO signal and the idler) were unequal and we assigned the ‘pump power’ to a geometric mean of the powers of the two beams. The best fit is a straight line with a slope of 2, which indicates that the THz output is linear with respect to the product of the powers of the two pump beams. The conversion efficiency was about 40% of theoretical²⁵; the discrepancy can be accounted for by the beam clipping, water vapor absorption at THz frequencies, and possible uncertainty in THz detector calibration. Overall, experiments with ps pulses confirm predictions of theory that one can get the same THz efficiency per μJ of pump pulse energy for both ps and fs pulses.

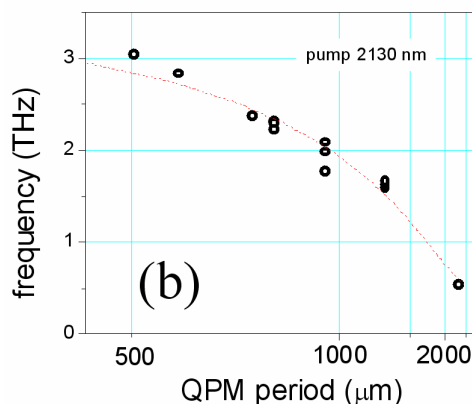


Fig.4. THz tuning curve: central THz frequency as a function of the GaAs QPM period. Dotted line – best polynomial fit.

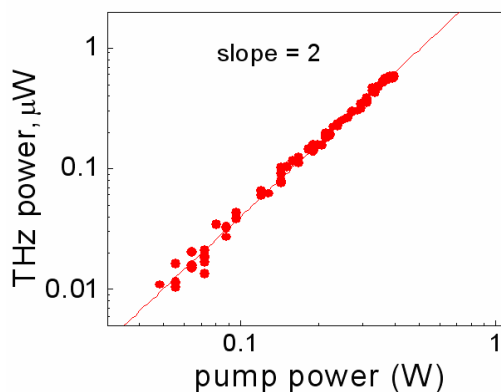


Fig.5. THz average power versus average pump power for a 5-mm-long OP-GaAs sample with the QPM period 704 μm and the central frequency of 2.2 THz. Straight line is the best fit.

6. INTRACAVITY THZ GENERATION, SRO

By placing the QPM GaAs inside the OPO cavity, one can take the advantage of resonant enhancement of the pump optical power near 2- μm wavelength. As we have shown experimentally, this enhancement can be a factor of 10-100, depending on the intracavity loss. In the case of single resonant OPO (SRO), only one wave is enhanced, while in the doubly resonant OPO (DRO), both waves are enhanced and the total THz efficiency can be boosted by a factor of > 100 .

With the AR-coated 6-mm-long DB-GaAs crystal (QPM period 504 μm) inside the SRO cavity and optical beams size at the DB-GaAs crystal of $\sim 200 \mu\text{m}$, we generated 50 μW of THz output at 2.9 THz. To extract the THz output radiation, we used an off-axis parabolic mirror with a 3-mm hole, to transmit resonating optical beam.

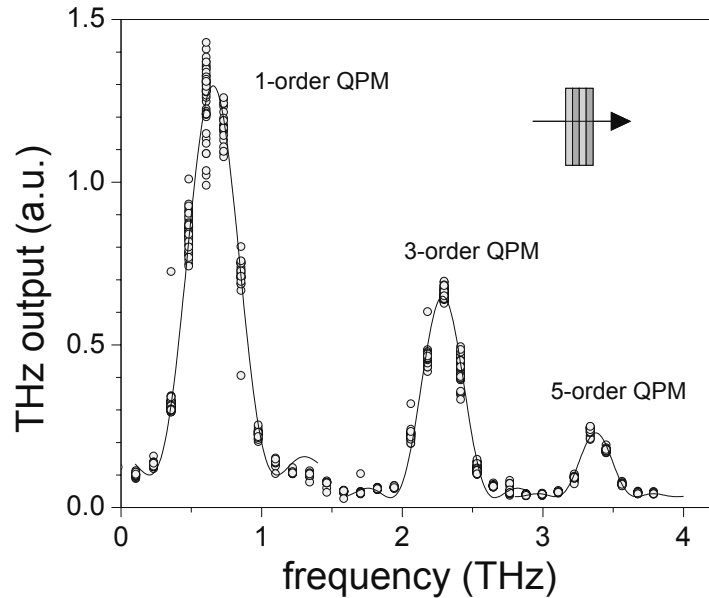


Fig. 6. THz output as a function of frequency, in the case of intracavity THz generation using a GaAs stack consisting of four 1-mm $\langle 110 \rangle$ optically-contacted plates. The peaks correspond to the 1-st, 3-rd and 5-th order QPM in GaAs. Solid curves are sinc^2 best fits.

We also used an optically-contacted GaAs in this experiment. A stack consisting of four 2-inch-diameter 1-mm-thick optically-contacted plates was mechanically robust and had optical transmission of 99% at $\lambda=2 \mu\text{m}$ after AR coating. The THz output as a function of the beat note frequency (tuned by changing the PPLN temperature) for the SRO case with the QPM GaAs inside the cavity is shown on Fig. 6. The three peaks correspond to the 1-st, 3-rd and 5-th order QPM in GaAs. Solid curves are sinc^2 best fits with the values for the peak position (FWHM) of 0.66 (0.39), 2.29 (0.33) and 3.38 (0.76) THz correspondingly. Potentially, such a 3-color THz source can be a useful tool for spectrally-selective THz imaging.

7. INTRACAVITY THZ GENERATION, DRO

Schematic of the setup for THz generation using a QPM GaAs inside the cavity of a doubly-resonant type-II PPLN OPO (DRO) is shown on Fig. 7. Two polarizers and two separate sets of end mirrors were used to resonate simultaneously the signal and the idler wave. The DRO configuration employed a special linear cavity design, which avoided back-conversion of the signal and idler in the PPLN (arm lengths between polarizers and end mirrors were made unequal for 's' and 'p' polarizations). For intracavity THz generation, we used an AR-coated 6-mm-long DB-GaAs crystal with a QPM period of 504 μm . As before, an off-axis parabolic mirror with a hole inside was used to extract the

THz output radiation. As a THz filter, we have used black polyethylene, and as a THz detector – a room temperature DLaTGS pyroelectric detector from Bruker. The average THz power at 2.9 THz was measured to be 1 mW, in a diffraction-limited beam (Fig. 8). In this case, we took the full advantage of resonant enhancement of both signal and the idler waves. However, special stabilization of one of DRO mirrors was needed for locking the cavity modes. To accomplish that, we have used the ‘dither-and-lock’ technique consisting of a piezo actuator at one of the end mirrors, a 2- μm photodetector and feedback electronics.

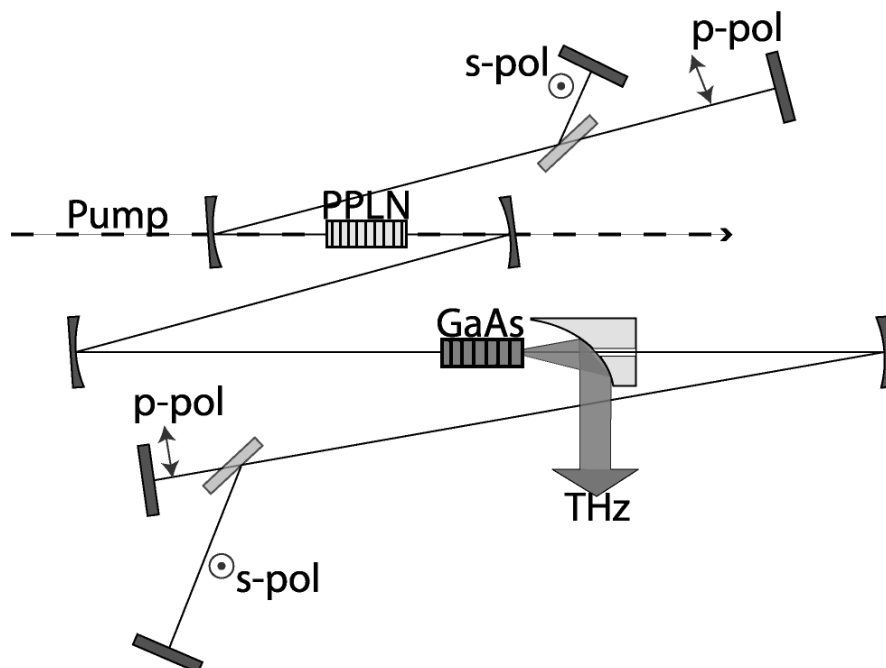


Fig. 7. Setup for THz generation using a QPM GaAs inside the cavity of a near –degenerate synchronously-pumped doubly-resonant type-II PPLN OPO. Off-axis parabolic mirror with a hole inside is used to extract the THz output radiation.

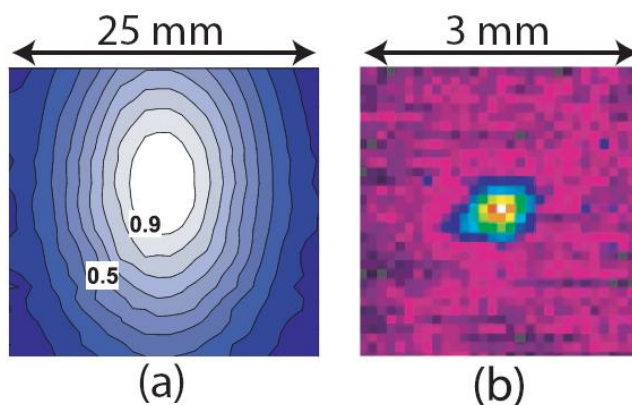


Fig. 8. (a) The collimated THz-beam intensity profile reconstructed from scanning knife- edge measurements. (b) The focused (Picarin $f = 5$ cm lens, L2) THz-beam intensity profile measured by a room-temperature pyroelectric camera (1 pixel = $100 \mu\text{m} \times 100 \mu\text{m}$).

8. CONCLUSION

We demonstrate a new source of frequency-tunable narrow-bandwidth (100-200 GHz) THz wave packets based on parametric down-conversion process in quasi-phase-matched GaAs. As a pump, we used the signal and idler waves of a picosecond near-degenerate OPO. We consider intracavity THz wave generation to be the most efficient way of producing THz output. This allowed us to achieve 1 mW of THz average power at room temperature, with $\sim 10^{-4}$ optical-to-THz conversion efficiency and potential scalability to 100 mW. This work was sponsored by DARPA under AFOSR Grant FA9550-04-1-0465.

REFERENCES

- ¹ F. Zernike, Jr., and P. R. Berman, "Generation of far infrared as a difference frequency," *Phys. Rev. Lett.* **15**, 999-1002 (1965).
- ² T. J. Bridges and A. R. Strnad, Submillimeter wave generation by difference-frequency mixing in GaAs, *Appl. Phys. Lett.* **20**, 382-4 (1972).
- ³ B. Lax, R.L. Aggarwal, G. Favrot, Far-infrared step-tunable coherent radiation source: 70 μm to 2 mm, *Appl. Phys. Lett.* **23**, 679-681 (1973).
- ⁴ W. Shi, Y. J. Ding, N. Fernelius, K. Vodopyanov, Efficient, tunable, and coherent 0.18–5.27-THz source based on GaSe crystal, *Opt. Lett.* **27**, 1454-6 (2002).
- ⁵ Y. Sasaki, Y. Avetisyan, K. Kawase, H. Ito, Terahertz-wave surface-emitted difference frequency generation in slant-stripe-type periodically poled LiNbO₃ crystal, *Appl. Phys. Lett.* **81**, 3323-25 (2002).
- ⁶ I. Tomita, H. Suzuki, H. Ito, H. Takenouchi, K. Ajito, R. Rungsawang, Y. Ueno, Terahertz-wave generation from quasi-phase-matched GaP for 1.55 μm pumping, *Appl. Phys. Lett.* **88**, 071118-1–071118-3 (2006).
- ⁷ M.A. Piestrup, R.N. Fleming, R.H. Pantell, Continuously tunable Submillimeter wave source, *Appl. Phys. Lett.* **26**, 418-421 (1975)
- ⁸ K. Kawase, M. Sato, T. Taniuchi, H. Ito, Coherent tunable THz-wave generation from LiNbO₃ with monolithic grating coupler, *Applied Physics Letters* **68**, 2483-85 (1996)
- ⁹ T. J. Edwards, D. Walsh, M. B. Spurr, C. F. Rae, M. H. Dunn, P. G. Browne, Compact source of continuously and widely tunable terahertz radiation, *Opt. Express* **14**, 1582-4 (2006)
- ¹⁰ L. Xu, X.-C. Zhang, and D. H. Auston, "Terahertz beam generation by femtosecond optical pulses in electro-optic materials," *Appl. Phys. Lett.* **61**, 1784-1786 (1992).
- ¹¹ Y.-S. Lee, T. Meade, V. Perlin, H. Winful, T. B. Norris, A. Galvanauskas, "Generation of narrow-band terahertz radiation via optical rectification of femtosecond pulses in periodically poled lithium niobate," *Appl. Phys. Lett.* **76**, 2505-7 (2000)
- ¹² C. Weiss, G. Torosyan, Y. Avetisyan, and R. Beigang, Generation of tunable narrow-band surface-emitted terahertz radiation in periodically poled lithium niobate, *Opt. Lett.* **26**, 563-565 (2001)
- ¹³ A. Stepanov, J. Kuh, I. Kozma, E. Riedle, G. Almási, and J. Hebling, Scaling up the energy of THz pulses created by optical rectification, *Opt. Express* **13**, 5762-5768 (2005).
14. Peter H. Siegel, Terahertz Technology, *IEEE Transactions on Microwave Theory and Techniques* **50**, 910-28 (2002).
15. T. J. Carrig, G. Rodriguez, T. S. Clement, and A. J. Taylor, Scaling of terahertz radiation via optical rectification in electro-optic crystals, *Appl. Phys. Lett.* **66**, 121-3 (1995).
16. A. G. Stepanov and J. Kuhl, I. Z. Kozma and E. Riedle, G. Almási and J. Hebling, Scaling up the energy of THz pulses created by optical rectification, *Optics Express* **13**, 5762 – 68 (2005).

17. Y.-S. Lee, T. Meade, V. Perlin, H. Winful, T. B. Norris, and A. Galvanauskas, Generation of narrow-band terahertz radiation via optical rectification of femtosecond pulses in periodically poled lithium niobate, *Appl. Phys. Lett.* **76**, 2505-2507 (2000).
18. Y.-S. Lee, T. Meade, M. DeCamp, T. B. Norris, and A. Galvanauskas, Temperature dependence of narrow-band terahertz generation from periodically poled lithium niobate, *Appl. Phys. Lett.* **77**, 1244-1246 (2000).
- ¹⁹ I. Tomita, H. Suzuki, H. Ito, H. Takenouchi, K. Ajito, R. Rungsawang, and Y. Ueno, "Terahertz-wave generation from quasi-phase-matched GaP for 1.55 μm pumping," *Appl. Phys. Lett.* **88**, 071118-1–071118-3 (2006).
- ²⁰ K. L. Vodopyanov, M. M. Fejer, X. Yu, J. S. Harris, Y.-S. Lee, W. C. Hurlbut, V. G. Kozlov, D. Bliss, C. Lynch, Terahertz wave generation in quasi-phase-matched GaAs, *Appl. Phys. Lett.* **89**, 141119-1 - 141119-3 (2006)
- ²¹ G. Imeshev, M. E. Fermann, K. L. Vodopyanov, M. M. Fejer, X. Yu, J. S. Harris, D. Bliss, C. Lynch, "High-power source of THz radiation based on orientation-patterned GaAs pumped by a fiber laser", *Opt. Express* **14**, 4439-4444 (2006)
- ²² for example, GaAs has absorption coefficient which is less than 5 cm^{-1} at 0–3 THz. A. Mayer, F. Keilmann, Far-infrared nonlinear optics. I. $\chi^{(2)}$ near ionic resonance, *Phys. Rev. B* **33**, 6954-61 (1986).
- ²³ L. A. Gordon, G. L. Woods, R. C. Eckardt, R. K. Route, R. S. Feigelson, M. M. Fejer, and R. L. Byer, Diffusion-bonded stacked GaAs for quasi-phases-matched second-harmonic generation of a carbon dioxide laser, *Electron. Lett.* **29**, 1942 - 1944 (1993).
- ²⁴ L. A. Eyres, P. J. Tourreau, T. J. Pinguet, C. B. Ebert, J. S. Harris, M. M. Fejer, L. Becouarn, B. Gerard, and E. Lallier, All-epitaxial fabrication of thick, orientation-patterned GaAs films for nonlinear optical frequency conversion, *Appl. Phys. Lett.* **79**, 904 – 906 (2001).
- ²⁵ K. L. Vodopyanov, "Optical generation of narrow-band terahertz packets in periodically inverted electro-optic crystals: conversion efficiency and optimal laser pulse format," *Opt. Express* **14**, 2263-2276 (2006)
- ²⁶ W. C. Hurlbut, Yun-Shik Lee, K. L. Vodopyanov, P. S. Kuo, M. M. Fejer, Multi-photon absorption and nonlinear refraction of GaAs in the mid-infrared, *Optics Letters* (in press)